doi:10.1017/S1431927617009540
Microsc. Microanal. 23 (Suppl 1), 2017

Interfacial Strain Mapping and Chemical Analysis of Strained-Interface Heterostructures by Nanodiffraction and Electron Energy-Loss Spectroscopy

William J. Bowman[1,2,3], Sebastian Schweiger[2], Reto Pfenninger[2,5], Ehsan Izadi[1], Amith Darbal[4], Jennifer L.M. Rupp[2,5] and Peter A. Crozier[1]

[1]. School for Engineering of Matter, Transport and Energy, Arizona State University, Tempe, AZ, USA
[2]. Electrochemical Materials Group, ETH Zürich, Switzerland
[3]. Laboratory for Electrochemical Interfaces, MIT, Cambridge, MA, US
[4]. AppFive LLC, Tempe, AZ, USA
[5]. Department of Materials Science and Engineering, MIT, Cambridge, MA, USA

Strain engineering is a relevant optimization route to introduce and/or optimize defects for mixed ionic-electronic conducting oxides. Interfacial strain control of electrical conductivity [1] and resistive switching [2] was reported for sideways-contacted $Gd_{0.1}Ce_{0.9}O_{2-\delta}|Er_2O_3$ (GCO|ERO) 'microdot' heterostructures with alternating monolayers of insulating ERO and mixed-conducting GCO, whose lattice mismatch yielded compressive strain in the GCO layers. Here we explore these and other GCO heterostructures with alternative straining oxides that impart varying degrees of tensile strain on GCO, such as $Bi_4NbO_{8.5}$|GCO (BNO|GCO). We apply local strain and chemical mapping, along with high resolution imaging in the TEM and scanning TEM (STEM) to provide nanoscale insights regarding strained heterostructure design.

We use Raman microscopy to determine the average strain state of the heterostructures, and employ a JEOL ARM200F with the ASTAR precession-enhanced electron nanodiffraction (PEND) system [3] to perform local strain mapping, resolving lattice distortion in the heterolayer systems at the nanometer scale. These strain data are correlated with interface atomic structure, composition and electronic structure characterized by high resolution imaging and electron energy-loss spectroscopy (EELS) in a scanning TEM (STEM).

The magnitude of overall in-plane strain was found to increase with the number of heterointerfaces for the ERO and BNO systems, Fig. 1a. These average strain data were corroborated by local strain mapping, e.g. Figure 1c, which exemplifies strain mapping on the BNO|GCO heterostructure system. EELS analysis was performed in addition to strain mapping, exemplified in Fig. 2 for BNO|GCO. In this case asymmetric interface growth wherein cation distributions varied from one interface to the next was observed, Fig. 2a. Characterization of atomic-level structure and composition in these systems, e.g. Fig. 2b, provides nanoscale insights regarding strained heterostructure design [4].

References:
[1] S. Schweiger, M. Kubicek, F. Messerschmitt, F. Murer, J.L.M. Rupp. ACS Nano 8 (2014) 5032
[2] S. Schweiger, R. Pfenninger, W.J. Bowman, U. Aschuauer, J.L.M. Rupp. Adv. Mat. (In press)
[3] A. Darbal, R.D. Narayan, C. Vartuli, G. Lian, *et al.*, Microsc. & Microanal. **19:S2** (2013), 702
[4] W.J. Bowman, S. Schweiger, E. Izadi, A.D. Darbal, J.L.M. Rupp, P.A. Crozier. (In preparation)
[5] We gratefully acknowledge access to the John M. Cowley Center for High Resolution EM and the Southwestern Center for Aberration-Corrected Electron Microscopy at ASU. W.J.B. was a Swiss Government Excellence Scholarship holder for the academic year 2015-2016 (ESKAS No. 2015.1183); he would like to acknowledge financial support of the US NSF's Graduate Research Fellowship

Program (under grant number DGE-1311230), and the US NSF's Graduate Research Opportunities Worldwide grant. P.A.C. and W.J.B. gratefully acknowledge support of NSF grant DMR-1308085. This work was supported by the Swiss NSF under the project numbers of 155986 (SNSF (ERC) starting grant) and 138914. In particular, we wish to acknowledge Qianlang Liu for her support during operation of the Nion UltraSTEM.

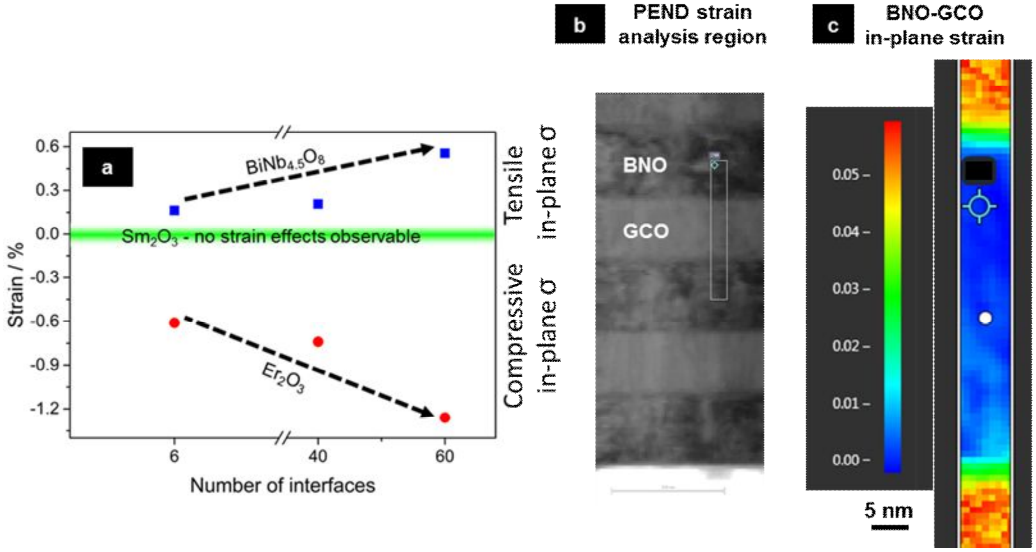

Figure 1. (a) Average in-plane strain analyzed by Raman microscopy for the different straining oxides studied here. (b) PEND local strain mapping region in the GCO-BNO heterostructure. (c) In-plane strain map was acquired in the region outlined in (b); colored scale bars indicate fractional strain relative to the reference point—assumed to be unstrained—indicated by the white dot in the GCO layer.

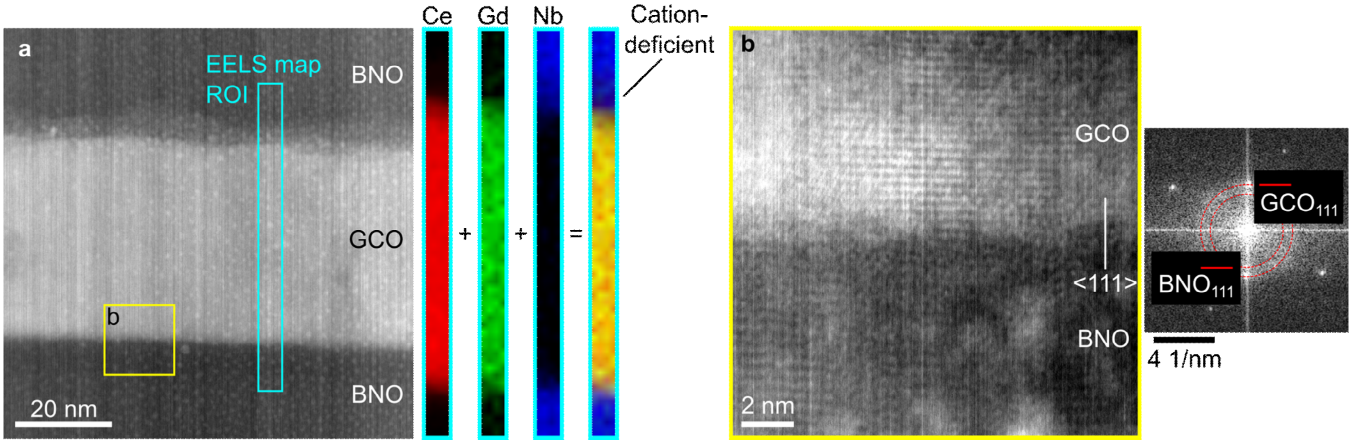

Figure 2. Local analysis of interface chemistry, composition (a), and structure (b) was performed using STEM imaging and EELS, as exemplified for the GCO-BNO heterostructure. (a) EELS analysis indicated asymmetric cation distribution in this heterostructure system, with a deficiency in Ce, Gd, and Nb cations present at the top interface (see integrated EELS core-loss signal maps at right). Bi enrichment was detected in these interfacial regions deficient in Ce, Gd and Nb cations. (b) Aberration-corrected STEM image confirming highly oriented, pseudo-epitaxial growth at the lower interface, see diffractogram at right. (b) was acquired from outlined region in (a) labeled 'b'. Data acquired with an aberration-corrected Nion UltraSTEM100.